PROCEEDINGS OF SCIENCE

A novel approach for $\overline{He}$ research in cosmic rays with neural networks

Francesco Rossi,[a,b,*] **Greta Brianti**[a,b,c,d] **and Paolo Zuccon**[a,b]

[a] *Department of Physics, University of Trento,*
Via Sommarive 14, Trento, Italy
[b] *INFN-TIFPA,*
Via Sommarive 14, Trento, Italy
[c] *Fondazione Bruno Kessler,*
Via Sommarive 18, Trento, Italy
[d] *CERN,*
Espl. des Particules 1/1211, 23 Genève, Switzerland
E-mail: francesco.rossi-9@unitn.it, greta.brianti@unitn.it, paolo.zuccon@unitn.it

Anti-nuclei heavier than $\overline{D}$ are unlikely to be formed during cosmic rays (CRs) propagation, as confirmed by the PHOENIX and ALICE collaborations. $\overline{He}$ observations could be related to Dark Matter interactions or to a primordial origin. Dedicated experiments must possess high charge sign discrimination to observe $\overline{He}$ due to the He abundance in CRs. Detector's effects, such as the rigidity resolution and the internal interactions, may lead to misidentifying matter as antimatter, producing a dominant background over rare signal candidates. In this work, we developed a Monte Carlo simulation to mimic the response of an AMS-02-like detector, identifying several phenomena that misidentify He as $\overline{He}$. The performances of a fully connected neural network, trained over diverse sources of charge sign confusion, are presented.

42nd International Conference on High Energy Physics (ICHEP2024)
18-24 July 2024
Prague, Czech Republic

*Speaker

PoS(ICHEP2024)747

1. Introduction

The search for antimatter in space addresses fundamental questions such as the origin of the matter-antimatter unbalance and the nature of Dark Matter (DM). Antinuclei heavier than $\overline{D}$ are unlikely to be formed during cosmic rays (CRs) propagation, as confirmed by the PHOENIX [1] and ALICE [2] collaborations. Especially at low energies, i.e. below 1 GeV/N the expected fluxes due to astrophysical sources are suppressed [3]. $\overline{He}$ is a possible golden channel, as any enhanced detection of such antinuclei might be related to DM annihilations or some primordial origin. $\overline{He}$ to He nuclei production ratio is $\sim 10^{-9}$, therefore dedicated experiments must possess high charge sign discrimination to observe $\overline{He}$ due to the He abundance in CR.
One of the experiments that is sensible to antihelium is the Alpha Magnetic Spectrometer (AMS-02). AMS-02 is a state-of-the-art particle physics detector currently operating on the International Space Station (ISS) [4].
This work aims to study the expected helium background and develop a classifier for recognising different charge confusion sources. For this reason, we developed a Monte Carlo (MC) simulation of an AMS-like detector, implementing only part of the AMS-02 subdetectors, focusing on the silicon tracker (TRK), the time of flight (TOF) and the anti-coincidence system (ACC) as shown in figure 1. These subdetectors were chosen because they reconstruct important physical quantities such as particle velocity, rigidity (p/Z), charge and possible interaction products. Moreover, they discriminate between charged confused events.

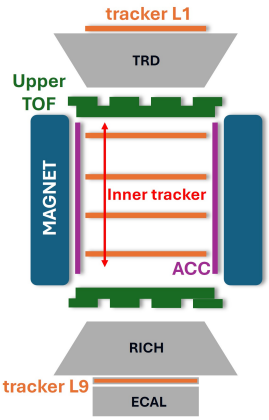

	He	$\overline{He}$
TRD	⌐	⌐
TOF	⌐⌐	⌐⌐
TRK	(	(
ACC	/⌐	/⌐
RICH	○	○
ECAL	⌐⌐	⌐⌐

Figure 1: The left image shows a pictorial cut view of the AMS-02 detector [4], the coloured subdetectors correspond to the sensible elements implemented in our MC toy. The right table shows how particles and antiparticles interact within each subsystem.

2. Sources of charge confusion

To investigate how helium nuclei can be misidentified as antihelium a MC sample of ^4He nuclei was simulated, and only nuclei with negative reconstructed rigidities were selected. Three different sources of charge confusion have been identified: spillover, inelastic and elastic interactions. A sample of representative events for each one of these sources was selected. These samples are used to train a Fully Connected Neural Network (FCNN) in recognising different backgrounds.

2.1 Spillover

Spillover is a consequence of the silicon tracker finite resolution. The tracker measures directly the inverse of rigidity, as shown in figure 2a. The mean value of $\frac{1}{R}$ [GeV^{-1}] distribution shifts towards zero when the generated rigidities increase, causing the tail of the distribution to spill over negative values. The width of the distribution corresponds to the tracker resolution and is related to the probability of reconstructing the rigidity with the wrong sign. To identify pure spillover events, the MC true information was used selecting only primary nuclei reconstructed with negative rigidity and without any interaction within the inner tracker. The inner tracker is the central part of the silicon tracker, and it measures the position of the bending particles within the magnetic field. As visible in figure 2a, spillover should be relevant, especially at high rigidities, i.e. energies. The migration matrix for the spillover sample, showing the logarithmic value of the measured rigidities on the horizontal axis and the logarithmic value of the generated rigidities on the vertical axis (figure 2b), serves as a crosscheck for the selection criteria quality. As expected the bulk of the selected events are high-energy events.

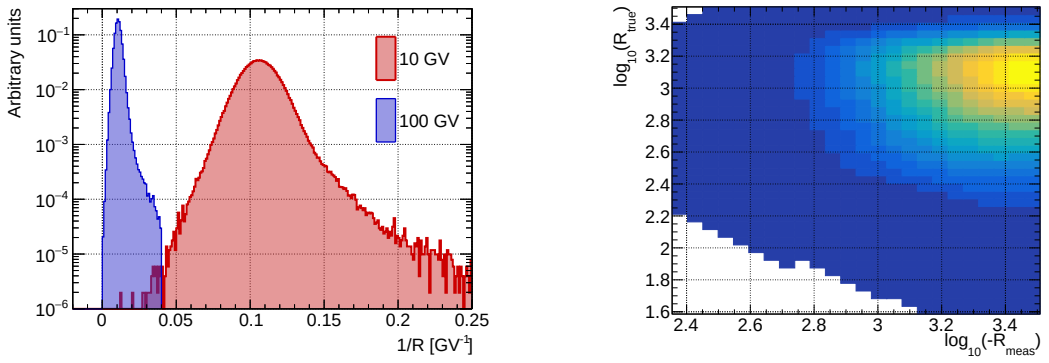

(a) **(b)**

Figure 2: Figure 2a shows the inverse rigidity distributions for two different categories of events: 10 GV and 100 GV generated rigidity. Figure 2b shows the reconstructed rigidities logarithmic values against the generated rigidities logarithmic values. As expected, the bulk of the selected sample consists mainly of high-energy events.

2.2 Inelastic and elastic interactions

Inelastic and elastic interactions affect the rigidity measurement if they occur within the inner tracker. During these interactions, the primary particle may vanish (inelastic) or change direction modifying its original path. Samples of primary nuclei interacting inelastically and elastically were selected using the MC truth asking for the interaction to occur within the the inner tracker volume. Figure 3 reports the scattering angle within the elastic scattering sample.

3. Fully Connected Neural Network classifier

The Fully Connected Neural Network (FCNN) classifier is based on pytorch libraries. It is composed of 4 linear layers, the first with 12 nodes, the second and the third with 32 nodes and the last layer

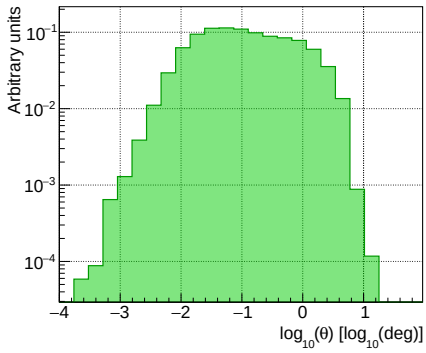

Figure 3: Logarithmic value of the primary particle scattering angle due to an elastic interaction. The selected events interact elastically within the silicon tracker, affecting the rigidity measurement.

with 3 nodes. The classifier is based on an Adam optimizer, with a learning rate of $1.0 \cdot 10^{-3}$ and a batch size of $5.0 \cdot 10^{3}$ events. The output of the network is a 3 elements vector, each element corresponds to the probability that a given event belongs to one of the three classes (spillover, inelastic and elastic interactions). The maximum value of the output vector is used to determine the class predicted by the model.

The loss function used is a Cross-Entropy for multiclass classification. The classifier is trained on a dataset composed of $7 \cdot 10^{5}$ events. Such a sample is balanced, meaning each charge confusion source has $1/3$ of the total training sample. The validation dataset is independent of the training one, is balanced and has $3 \cdot 10^{5}$ events. The FCNN receives as input 12 features, scaled on the training dataset. Therefore, each feature values are included between 0 and 1. The full list of the input features, with their description is presented in table 1. The correlation between the chosen input features is presented in figure 4.

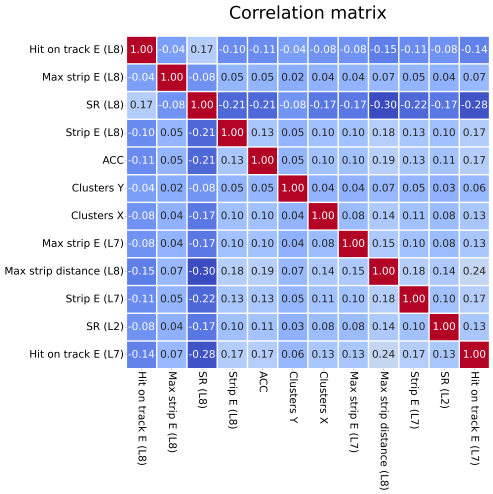

Figure 4: The correlation matrix for the 12 features given as input to the FCNN classifier.

Name:	**Description:**
L8 distance from track hit	Distance between track hit and strip with max energy deposit on layer 8.
L8 strip E ratio	Ratio between strip energy deposition and its neighbouring 10 strips, on layer 8.
L3-L8 number of hits Y	Number of hits in layers 3-8 inner tracker Y side.
L8 track hit E deposit	Track hit energy deposition on layer 8.
L8 E deposit	Total energy deposition on layer 8.
L7 max strip E deposit	Max energy deposit on a single strip on layer 7.
L2 strip E ratio	Ratio between strip energy deposition and its neighbouring 10 strips, on layer 2.
L3-L8 number of hits X	Number of hits in layers 3-8 inner tracker X side.
L8 track hit E deposit	Track hit energy deposition on layer 7.
L7 E deposit	Total energy deposition on layer 7.
Number of fired ACC	Number of fired ACC.
L8 max strip E	Max energy deposit on a single strip on layer 8.

Table 1: List of the input features used to train the FCNN classifier. The number of layers refers to the silicon tracker layer number.

4. Classifier performance

Figure 5a presents the output of the classifier, using the discriminants expression, divided by classes. The discriminants are defined as follows:

$$D_i = \log\left[\frac{p_i}{(p_j \cdot f_j) + (p_k \cdot f_k)}\right] \tag{1}$$

where p_i, p_j and p_k are the predicted probabilities that a given event belongs to one of the three classes. The $f_i = f_j = f_k = \frac{1}{3}$ are the event fraction belonging to each class.
The overall performance can be evaluated by estimating the area under the Receiver-Operating-Characteristic (ROC) curve as presented in figure 5b. The dashed black line corresponds to the expected ROC for a random classifier, whilst a perfect classifier should have an Area Under the Curve (AUC) equal to 1. All three colour lines stand above the bisector. The best results are achieved in recognising the inelastic interactions with an AUC = 0.999, whilst the spillover and elastic classes are more difficult to identify AUC = 0.856 and 0.867 respectively.

5. Conclusion

Using a Monte Carlo sample of ^4He nuclei, a study of the events wrongly reconstructed with negative rigidities has been carried out. Three different sources of charge confusion have been

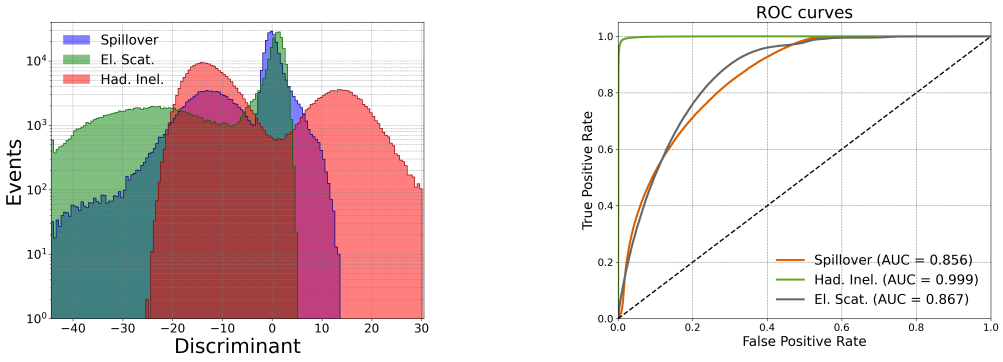

(a) **(b)**

Figure 5: Distribution of the discriminant value described in equation 1 for each of the three classes 5a. ROC curves divided per class. The classifier recognises well the inelastic interactions, while the performance for spillover and the elastic scattering events are worse 5b.

identified within the available statistics, corresponding to spillover events, and inelastic and elastic interactions. A FCNN classifier has been trained to distinguish between these charge confusion sources. The classifier performs well in recognising the inelastic interactions, but the prediction deteriorates for elastic and spillover events. As prospects, it will be necessary to study the features dependency on rigidity and investigate the classifier behaviour. Assuming a satisfying agreement between MC and real data, applying the same selections and classifier it will be possible to estimate $4^H e$ background reduction for the research of $\overline{He}$ in cosmic rays.

Acknowledgments

This publication was produced while F.R. attending the PhD program in Space Science and Technology at the University of Trento, Cycle XXXVIII, with the support of a scholarship financed by the Ministerial Decree no. 351 of 9th April 2022, based on the NRRP-funded by the European Union - NextGenerationEU - Mission 4 "Education and Research", Component 1 "Enhancement of the offer of educational services: from nurseries to universities" - Investment 4.1 "Extension of the number of research doctorates and innovative doctorates for public administration and cultural heritage" - CUP E63C22001340001

References

[1] PHENIX Collaboration collaboration, *Deuteron and antideuteron production in* Au + Au *collisions at* $\sqrt{s_{NN}}$ = 200 GeV, *Phys. Rev. Lett.* **94** (2005) 122302.

[2] S. Acharya, D. Adamová, A. Adler, J. Adolfsson, G. Aglieri Rinella, M. Agnello et al., *Measurement of anti-3he nuclei absorption in matter and impact on their propagation in the galaxy*, *Nature Physics* **19** (2022) 61–71.

[3] M. Korsmeier, F. Donato and N. Fornengo, *Prospects to verify a possible dark matter hint in cosmic antiprotons with antideuterons and antihelium*, *Phys. Rev. D* **97** (2018) 103011 [1711.08465].

[4] S. Ting, *The alpha magnetic spectrometer on the international space station*, *Nuclear Physics B - Proceedings Supplements* **243-244** (2013) 12.